THE JOURNAL OF PHYSICAL CHEMISTRY B

pubs.acs.org/JPCB Article

Structural and Thermophysical Anomalies of Liquid Water: A Tale of Molecules in the Instantaneous Low- and High-Density Regions

Adyasa Priyadarshini,[§] Aritri Biswas,[§] Debashree Chakraborty,* and Bhabani S. Mallik*

Cite This: *J. Phys. Chem. B* 2020, 124, 1071−1081 Read Online

ACCESS | Metrics & More | Article Recommendations

ABSTRACT: Water is believed to be a heterogeneous liquid comprising multiple density regions that arise because of the presence of interstitial molecules and can be differentiated by their structure as well as the existence of hydrogen-bonded pairs with varying strengths. First-principles molecular dynamics studies were performed at six different temperatures to investigate the effect of temperature on the thermophysical, structure, dynamics, and vibrational spectral properties of the water molecules using dispersion-corrected density functional theory. The variation of properties like density, cohesive energy, and compressibility with a change in temperature produces a trend that matches with the experiments and resembles the experimentally observed anomalous behavior. We explore the possibility of explaining the trends in calculated properties by analyzing the structure and dynamics of the water molecules in terms of instantaneous low- and instantaneous high-density regions that are found during the simulation time. The dynamics of these two types of water molecules were studied by calculating the lifetime from the proposed autocorrelation functions. The lifetime of formation of instantaneous low-density water is found to decrease with an increase in temperature, whereas the lifetime of instantaneous high-density water is found to be maximum at 298 K among all the considered temperatures. The presence of more interstitial water molecules is observed at this temperature. The signature of these water molecules is found in the radial distribution function, spatial distribution function, void distribution, configurational space, orientational dynamics, and spectral diffusion calculations. It is also found that around 298 K, these water molecules are present distinctively that mix up with the first and second solvation shells with the rise of the temperature. The outlook of the reported results can be extended to other thermodynamic conditions to explain some of the anomalous properties, which can be related to the presence of the interstitial molecules in water.

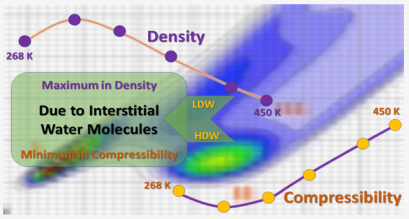

1. INTRODUCTION

A complete understanding of the various properties of water is far from our scientific and technological developments. The well-understood properties of water can give clues to the reasons for its many anomalous properties. At ambient conditions, it may behave like a normal molecule to be explored, but with a change in thermophysical conditions, like temperature and pressure, it behaves differently as compared to others. Density anomaly is one of such properties. Most liquids contract upon cooling, but the water does the contrary; it expands with a decrease in temperature. The anomalous behavior of water is not only found in density but also in isothermal compressibility, which is due to a lack of cooperative phenomena resulting from the anomalous fluctuations in density.[1] The isothermal compressibility decreases when temperature decreases for most of the liquid. For water, it is different; liquid water displays a minimum in isothermal compressibility at 320 K, and isothermal compressibility increases below this temperature.[2] This phenomenon occurs very rapidly in the supercooled region.[3] The anomalous fluctuation in density and isothermal compressibility is often explained by the cooperative effect of hydrogen-bonded water molecules.[4,5] The variation in the tetrahedral hydrogen-bonding environment is the key feature for water molecules to exhibit the peculiar behavior in both liquid and solid forms. Though the experimental and theoretical studies reveal that H_2O possesses the same coordination environment in both liquid and ice forms, it is found that liquid water contains a fraction of broken hydrogen-bonded water molecules.[6−11] The low- and high-density environment in a liquid state was identified by the neutron diffraction experiments.[12] With an increase in the pressure at 268 and 298 K temperatures, the structure of water was found to be dominated by a high-density nontetrahedral arrangement from the low-density tetrahedral arrangement.[13] The arrangement of low- to high-density molecules also arises due to the change in local hydrogen-bonding strength.[14−17] Variation of thermodynamic conditions, like temperature and pressure, leads to the differences in the structure, density, and voids of the systems. Woutersen and co-workers[6] reported two distinct species of water molecules in

Received: December 16, 2019
Published: January 21, 2020

https://dx.doi.org/10.1021/acs.jpcb.9b11596
J. Phys. Chem. B 2020, 124, 1071−1081

the liquid phase based on their observation on different time scales of orientational relaxation.[6] Sciortino and Fornili reported that water molecules of two different groups, "stably linked" and "unstably linked," exist, which can be identified by their hydrogen bond lifetime in a liquid state. These dynamically and structurally distinct groups of water molecules have a difference in bond stability, molecular mobility, and local order. The "stably linked" molecules were characterized by lower local density.[18] Thus, the change in the local hydrogen bond network affects the dynamic properties of water molecules. However, the anomalous reorientational dynamics of water molecules was not found to be linked with the presence of high-density and low-density water.[19] The presence of interstitial water molecules in between the first and second solvation shell is the main reason for the origin of two phases of water molecules. Based on the multiphase environment of water molecules, many anomalous properties of water molecules in the liquid state can be explained. In the supercooled region of water, these two types of water molecules are prevalent.[20−23] The structure of water at ambient conditions, which was traditionally considered as a homogeneous distribution of near-tetrahedral hydrogen-bonded structures, is challenged by recent studies based on X-ray Raman and conventional X-ray absorption spectroscopy[24,25] and X-ray emission spectroscopy[26] experiments. Various other experimental studies on liquid water, such as neutron scattering,[12,27] terahertz spectroscopy,[28] and ultrafast spectroscopy,[6,29] identified the multiphase water components. These studies suggested two distinct local structures: one with the tetrahedral structure and another with hydrogen-bonded distorted asymmetrical structures, which were present as minority and majority states in the system, respectively. Different types of voids were also reported for low- and high-density regions.[30] Our recent theoretical calculations suggest that the interstitial water molecules are found in the region of 2.70−3.35 Å according to the intermolecular oxygen−oxygen radial distribution function (RDF)[31] and other structural analysis. Very recently, water was described as a dynamic branched polymer chain from the investigation of structure and dynamics through classical molecular dynamics simulations.[32] It is expected that these interstitial water molecules are dynamically and spectroscopically different from the tetrahedrally hydrogen-bonded water molecules. The shifting of OH vibrational stretching frequency characterizes the hydrogen bonding strength in liquid water. The time scales of few femtoseconds observed in the vibrational spectral diffusion process are related to intact water−water hydrogen bonds, and the picoseconds time scales correspond to the breaking and making of hydrogen bonds.[33−36] This time-dependent property of water molecules was investigated by nonlinear vibrational spectroscopy.[6,37−41] The other experimental methods such as spectral hole-burning,[7,42−45] photon-echo peak shift spectroscopy,[46−50] two dimensional vibrational spectroscopy,[51−58] and other photon-echo experiments[59,60] were also used extensively to get the spectral diffusion of water molecules. Few theoretical calculations in HDO/D_2O or HDO/H_2O mixtures were also performed to understand the spectral diffusion process by constructing frequency−frequency time autocorrelation functions.[33,34,48,49,51,52,54,56,58,61−74] All these results are in qualitative agreement with the experimental results in terms of rapid initial decay in the range of ∼50−100 fs and slower decay of time scales of around 0.5−1 ps. The anomalous properties exhibited by liquid water are the macroscopic expression of the microscopic cooperative mechanism. In this respect, we performed first-principles molecular dynamics (FPMD) simulations of H_2O molecules at six different temperatures using Becke−Lee−Yang−Parr (BLYP)[75,76] exchange−correlation function with Grimme's D3[77] dispersion correction. The focus is to explore the existence of water molecules in the instantaneous low- and high-density regions and study their structural, dynamical, and spectral properties. We define the molecules in these different density regions as instantaneous low-density water (i-LDW) and instantaneous high-density water (i-HDW), as the configuration of the water molecules keeps on changing with the simulation time. These regions reflect the heterogeneous fluctuations of the system in time and space around its average value without representing an extended and compact state of liquid water. The understanding of the structural fluctuation of water molecules provides the details of the collective motion of water molecules. We aim to explore the effect of temperatures on the structure, density, isothermal compressibility, cohesive energy, distribution of interstitial molecules, and void space distribution of liquid water, in particular, the dynamics and vibrational spectra of i-LDW as well as i-HDW molecules. We also explore the possibility of explaining a few of the anomalous properties of water in terms of these molecules.

2. COMPUTATIONAL METHODOLOGY

We performed FPMD simulations of liquid water using the Quickstep[78] module implemented in CP2K[79] (www.cp2k.org) software package at 268, 298, 330, 350, 400, and 450 K temperatures. The Born−Oppenheimer molecular dynamics simulations were performed for each temperature with BLYP[75,76] exchange−correlation functional, together with van der Waals dispersion correction of Grimme's D3[77] method. Each simulation box contained 50 water molecules. GTH pseudopotentials[80,81] were used to treat the core electrons. For the Gaussian wave function, TZV2P basis set was used and the charge density cutoff 600 Ry was used for the auxiliary plane-wave basis.[82] The time step of 0.5 fs was used to propagate the trajectories. Periodic boundary conditions were applied in all *XYZ* directions. The starting geometries for FPMD simulation were taken from the force-field simulations, which were carried out with SPC/E[83] water models at the *NVT* ensemble. At the force-field simulation, pre-equilibration was done for 3 ns simulation run time with a density of 1000 kg m^{-3}. The geometry optimization was also carried out in CP2K before FPMD simulations. The FPMD simulations were carried out at the temperatures above at *NpT* ensemble at 1 atm pressure. Temperatures were controlled by the Nosé−Hoover chain thermostat,[84] whereas the pressure was controlled by the method explained by Mundy and co-workers.[85] Each system was equilibrated for 10 ps to stabilize the energy and volume of the system. After that, a 25 ps simulation run was carried out for each system at the *NpT* ensemble, and the last 20 ps simulation was used for obtaining the equilibrium simulation box length, which was used to calculate the density of each system. Using this box length, we performed simulations at the *NVT* ensemble for another 52 ps, and the last 50 ps simulated trajectory was used for the calculations.

https://dx.doi.org/10.1021/acs.jpcb.9b11596
J. Phys. Chem. B 2020, 124, 1071−1081

3. RESULTS AND DISCUSSION

3.1. Thermophysical Properties. Water being an anomalous liquid shows exceptionally different thermodynamic behavior than other common liquids.[86,87] In this section, we focus on the observed anomaly in essential properties such as density, cohesive energy, and isothermal compressibility calculated from the FPMD simulations, and the corresponding data obtained at six different temperatures at atmospheric pressure are presented in Figure 1. These are among a few properties, which show very different behavior with the change in thermophysical conditions as compared to other liquids. The density (Figure 1A) of water was calculated from the equilibrated average volume of the simulation box obtained from *NpT*-based FPMD methods. At ambient conditions, the BLYP-D3 with the TZV2P basis set electronic method predicts a higher density than the experimental one (997.04 kg m^{-3}) of water, and the differences in other temperatures are also observed.[88] We note that the experimental density maximum (999.973 kg m^{-3}) for water is observed at 277.15 K.[88] However, we did not perform the simulations at this temperature. Therefore, our reported value at 298 K should not be assumed as the density maximum for water. Overall, the trend obtained from our results at a limited number of temperatures is similar to the experimentally observed one. The accuracy of the reported results can be enhanced by various ways: long enough simulations time within the *NpT* ensemble, the addition of nuclear quantum effects, large charge density cutoff, and different functionals, as well as dispersion corrections. However, these factors for improving the accuracy of the thermophysical properties need more computational resources. We also assume that the observed deviation in density will extend to other properties reported in this study. In Figure 1B, we present the cohesive energy of liquid water at different temperatures. Cohesive energy (ΔU_{coh}) measures the strength of intermolecular forces, that is, the energy required to isolate a molecule, which is in interaction with identical molecules of the same substance.[89,90] Higher is the cohesive energy more is the resistance to be separated. For normal liquids, the cohesive energy decreases as temperature rises[91] because, with the rise in the temperature, the kinetic energy of the molecules increases due to a decrease in intermolecular forces. For the calculation of cohesive energy, we simulated water molecules in the isothermal−isochoric ensemble for different temperatures, followed by the simulation within the *NVT* ensemble. For an isolated system, we simulated one water molecule with the same average box length as obtained from the *NpT* simulation of water molecules corresponding to that temperature. The cohesive energy was calculated from the difference between the average energies of the water in the liquid and gas states. ΔU_{coh} is found to be 41.38 kJ mol^{-1} at 268 K, which increases to 44.8 kJ mol^{-1} as the temperature increases to 298 K; then it decreases with a further rise in the temperature. The cohesive energy at 298 K is found to be in good agreement with the experimental value[92] of 44.55 kJ mol^{-1}, and the trend obtained for ΔU_{coh} matches with the experimental results. The observed exceptionally high ΔU_{coh} between water molecules in the liquid state at ambient temperature and pressure is due to the strong hydrogen bond interactions between the water molecules, which leads to a high boiling point. Along with the density and cohesive energy, the anomalous behavior in isothermal compressibility is also observed with the change in temperature. The isothermal compressibility (κ_T) is a thermodynamic phenomenon that explains the relative change in volume as a response to change in pressure at constant temperature and is given by

$$\kappa_T = \frac{-1}{V}\left(\frac{\Delta V}{\Delta P}\right)_T \quad (1)$$

In Figure 1C, we show the compressibility of water obtained from the isothermal and isobaric ensemble-based simulations. We carried out *NpT* simulations with six different temperatures at atmospheric pressure. Experimental studies on the compressibility of water show relatively higher values below absolute zero. As the temperature rises, the compressibility decreases till 298 K then again rises with the rise of the temperature.[2,93] Most of the liquids show a linearly increasing trend for compressibility as temperature increases, but the same does not apply to water. At 268 and 298 K, the values of κ_T are 0.309 and 0.204 GPa^{-1}, respectively. The obtained values from our simulations show an error of ∼25% with respect to the experimentally reported values. Because our simulations were carried out with dispersion correction, there is a reduction in the values of κ_T. The dispersion-corrected functional produces satisfactory thermophysical properties within the accuracy level of the adopted electronic structure method as compared to experiments but show a significant deviation in the compressibility.[2] Similar results were also previously reported by Galli et al. by simulating water molecules with PBE functional with dispersion correction and PBE0 functional.[94] We observe the maximum in both the density and cohesive energy corresponding to the minimum in compressibility data at the same temperature. By comparing the trend obtained from variation in density with the temperature, it is seen that κ_T increases as density decreases. The minimum in compressibility values correlates with the maxima in density and cohesive energy. With an increase in density and cooperative nature, it is difficult to compress the water molecules, which results in low isothermal compressibility. In our current investigation, the thermophysical anomalies are observed primarily below 400 K, and water

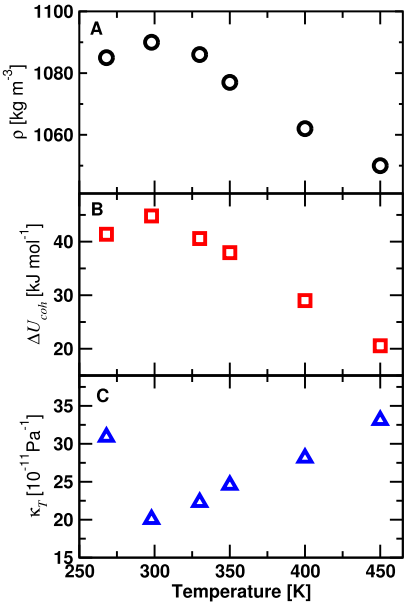

Figure 1. Thermophysical properties of water at various temperatures.

https://dx.doi.org/10.1021/acs.jpcb.9b11596
J. Phys. Chem. B 2020, 124, 1071−1081

molecules behave similarly to other liquids beyond this temperature for the thermophysical properties reported here. Therefore, we decided to consider these four temperatures for our further analysis of structure, dynamics, and spectral properties.

3.2. Structural Properties. The structural arrangement of water molecules with the variation of temperature is extracted from the intermolecular oxygen−oxygen and oxygen−hydrogen RDFs. Figure 2A shows the effect of the temperature on

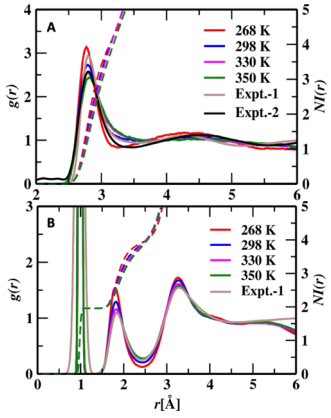

Figure 2. (A) RDF of the oxygen−oxygen distance correlation function of water molecules at different temperatures. (B) RDFs for oxygen−hydrogen pairs at different temperatures are shown. The experimental data is shown from neutron diffraction[95] (Expt-1) and X-ray[96] (Expt-2) experiments at 298 K.

oxygen−oxygen RDFs and the comparison of simulated data with the Neutron diffraction[95] and X-ray[96] experiment data of oxygen−oxygen RDF. The first peak of the O−O RDF profile occurs at 2.80 Å for all of the temperatures. The variation is observed in the positions of minima and height of the first peaks. The increase in temperature causes a decrease in the peak height and shifting the position of the first minima slightly toward the higher distances. The better agreement is observed in the position and height of the first peak at 298 K with the X-ray data. However, the depth of the minimum deviates that of the experiment. In Figure 2A, we also show the effect of temperature on number integrals (NIs) along with RDFs. With increasing temperature, we observe a slight change in the coordination number of water molecules. Figure 2B represents the O_w−H_w RDFs with the variation of temperature. The positions of maxima and minima of the peaks are invariant with the variation of temperatures. The NI values also do not change much on changing temperatures; only peak height decreases with increasing the temperature. We also calculated spatial distribution functions (SDFs) of oxygen atoms around the water molecule to check the effect of temperature on the three-dimensional structural properties. The calculated results of SDFs are shown in Figure 3, in which the density of oxygen atoms is shown in first and second solvation shells explicitly indicating two distinctive layers. The distances of the first and second solvation shells are taken from the corresponding RDFs. Compact oxygen clouds are observed at 268 K compared to the other temperatures both in first and second solvation shells. The oxygen clouds become more diffused at higher temperatures. Further, the effect of temperature on the structural property can be well understood from the contour plots (Figure 4) of the configurational space of water

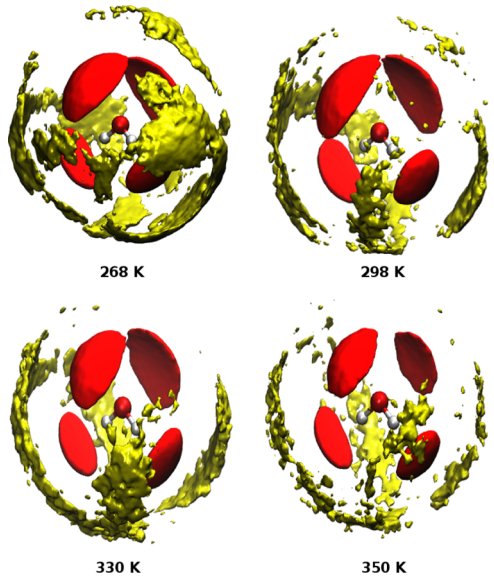

Figure 3. SDF of oxygen clouds around the water molecules in the first and second solvation shells at different temperatures.

molecules. In this figure, x-axis and y-axis represent intermolecular O−H and O−O distances, respectively. The contour in the figure indicates the probability distribution of each O−H and O−O intermolecular distances. The plot shows two distinctive regions (regions I and II) corresponding to the first and second solvation shells for all temperatures. In between the first and second solvation shells, interstitial sites are observed ranging between 2.7 and 3.35 Å (region III); the probability of finding water molecules is less in this region as compared to the other two regions. The intensity of this intermediate region, that is, interstitial sites, increases from 268 to 298 K. This indicates that the probability of finding some interstitial molecules increases at 298 K. At this temperature, the three regions are much distinctive as compared to 268 K, but on further increasing the temperature, the first and the second solvation shells mix up with the interstitial sites at 330 and 350 K. The interstitial water molecules are trapped within the distance range of 2.70−3.35 Å. Earlier, we showed that the high-density and low-density water molecules arise due to the presence of interstitial water molecules between the first and second solvation shells.[31] It would be interesting to see the change in the population and dynamics of these water molecules with the variation of temperature.

3.3. Population of i-HDW and i-LDW Molecules. The population of low-density and high-density water molecules is primarily distinguished by the presence of the interstitial molecules in between first and second solvation shells. Intermittent and chaotic motion of the hydrogen bond network was studied by Shiratani[14] employing molecular dynamics simulations. The author proposed that "individual water molecule alternatively goes through two different periods" by analyzing the fluctuation in the RDF, which is based on distances. The population analysis will give us an idea about the presence of i-HDW and i-LDW molecules with the change of the temperature quantitatively. In Figure 5A, we show the population distribution of the number of oxygen molecules present within a range of 3.35 Å from a central oxygen atom. If the numbers of coordinating oxygen molecules of water molecules are ≤ 4 and ≥ 5, the entities are considered as i-LDW and i-HDW, respectively. It can be noted here that

https://dx.doi.org/10.1021/acs.jpcb.9b11596
J. Phys. Chem. B 2020, 124, 1071−1081

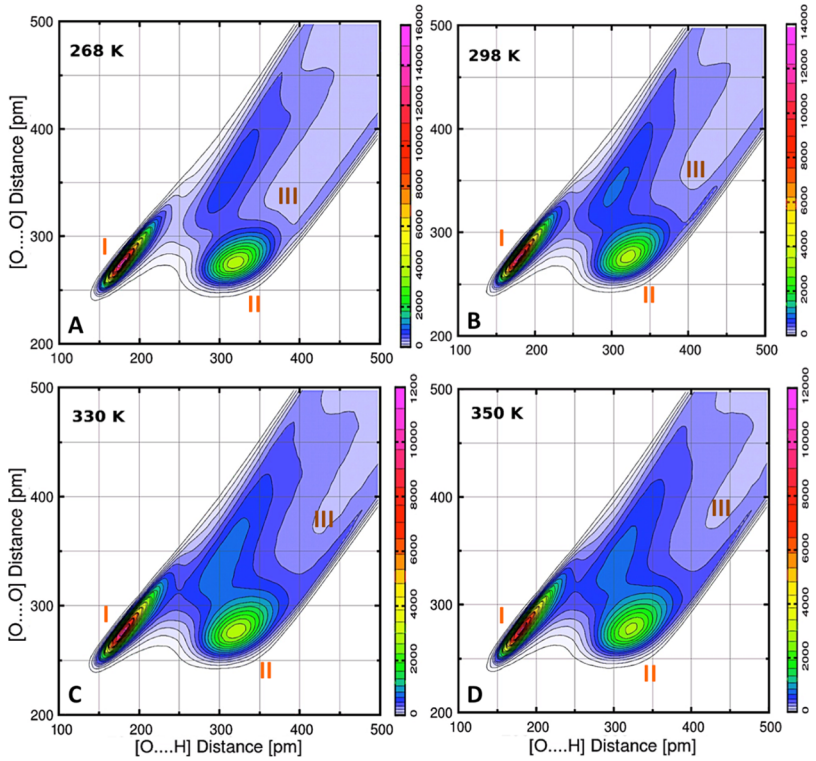

Figure 4. Configurational space of water molecules at different temperatures. The marked I, II, and III regions are the locations around which i-HDW and i-LDW molecules are found.

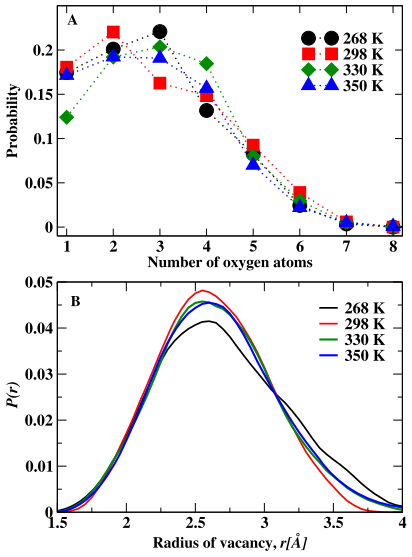

Figure 5. (A) Probability distribution of the number of oxygen molecules within a radius of 3.35 Å around the central oxygen atom at different temperatures. (B) Probability distribution of radius of vacancies at different temperatures.

we have to choose the cutoff for defining these types of molecules. Based on the choice of the cutoff, the distribution will be different. Ideally, these interstitial water molecules are placed in between the first and second solvation shells; so the cutoff distance may be near to the first minimum of $g(r)$. We reiterate that this distance may be different for various theoretical methods employed to simulate the water molecules. In our case, a value of 3.35 Å for the cut off is found to be a good condition for defining a dividing surface for i-LDW and i-HDW molecules at all the temperatures.

The probability of having two coordinated water molecules, that is, trimer within a radius of 3.35 Å is maximum for 298 K, whereas at 268 K, three coordinated water molecules are more probable. Our observations agree well with the fact that 80% of the hydrogen bonds in liquid water are broken and distorted; only 20% have a proper tetrahedral structure.[97] The probability of finding five and higher coordinated water molecules within a range of 3.35 Å is observed to be more in the case of 298 K as compared to other temperatures. The trend is as follows for other temperatures: 330−268 > 350 K. This shows that water has more probability of having interstitial molecules near the first solvation shell at 298 K. As the tetrahedrality has a relationship with the density maximum,[13,98] the presence of more population of tetrahedral and interstitial water molecules at 298 K can be correlated to the observed density maximum and subsequently to the observed anomaly in cohesive energy and isothermal compressibility.

3.4. Distribution of Voids at Various Temperatures.

Another way to analyze the structure of water is to investigate the free space, voids. We analyzed the voids in liquid water through the Voronoi polyhedra (VP) method, which is an efficient way to look into the structural details of the system. This property can be correlated to the discussed results in earlier subsections. It will be necessary for the current case of study to see whether we observe any temperature-dependent anomalous trend in the arrangement of the water molecules. From a set of configurations of atoms, we generated a tessellation in the three-dimensional space known as Voronoi tessellation, named after the scientist who invented the method.[35] The tessellation consists of repetitive units of the VP region of the atoms. The units are defined as the regions

https://dx.doi.org/10.1021/acs.jpcb.9b11596
J. Phys. Chem. B 2020, 124, 1071−1081

consisting of all points, which are nearer to the reference atom than any other atoms. The distance between the vertex of the VP and the atom minus the atom radius corresponds to the void radius. The other way of defining the tessellation is Delaunay tessellation. VP and Delaunay tessellation are complementary to each other. We took the coordinates of the oxygen atoms to generate the tessellation, and the Voronoi analysis was executed by the algorithm described in the earlier refs.[35,39] The plot of the probability distribution of the voids present in the different systems is shown in Figure 5B. Generally, it is seen that the probability distribution of voids gets broader[99,100] with an increase in temperature. However, we find a decrease in the average radius of vacancy as we go from 268 to 298 K, and then it increases to 330 K. Both the temperatures, 330 and 350 K, have similar distributions. When we go from 268 K, the density increases and then it decreases when we move toward a higher temperature, 330 K. Therefore, the density anomalous is also reflected in the void distribution of the system.

3.5. Orientation Profile of O−H Bond of Water Molecules. In this part, we discuss the reorientation profile of the O−H bond vectors of two layers; we expect the differences in orientation of OH vectors that originates from the change in local density. For orientation autocorrelation function (OACF) of the O−H bond vector, we used the O−O distance cutoff, that is, $r_{OO} < 2.7$ Å, to define layer 1 (L1) and 2.7 Å $< r_{OO} <$ 3.35 Å to define layer 2 (L2). The correlation function through second-order Legendre polynomial is given by

$$C_2(t) = P_2[u_{OH}(0)u_{OH}(t)] \tag{2}$$

where $u_{OH}(0)$ and $u_{OH}(t)$ are the orientation of the O−H vector at $t = 0$ and $t = t$, respectively. We fitted the decaying curve with the equation given by[101]

$$A \exp\left[-\left(\frac{t}{\tau_2}\right)^{\beta}\right] \tag{3}$$

The decay of correlation function and corresponding data are shown in Figure 6 and Table 1, respectively. At 268 K, the reorientation time in the L1 region (τ_2^{L1}) for the O−H bond vector is 33.57 ps and that in the L2 region (τ_2^{L2}) is 30.89 ps. Similarly τ_2^{L1} for 298, 330, and 350 K are 5.14, 2.38, and 1.58 ps, respectively. τ_2^{L2} values for 298, 330, and 350 K are 4.48, 2.07, and 1.42 ps, respectively. The difference between τ_2^{L1} and τ_2^{L2} decreases with an increase in temperature. With the rise in the temperature, the rate of making and breaking of hydrogen bonds increases and the two defined regions become less and less distinguishable. The τ_2^{L1} (=2.38 ps) obtained for 330 K is comparable to the calculated τ_2^{Bulk} (=2.6 ps) of an aqueous solution of trimethylammonium N-oxide at 323 K using BLYP-D3 functional. In the hydrophobic region, the movement of water is restricted, but the bulk water molecules behave as pure water.[102] Our results follow the experimental value of the reorientation time (2.5 ps) for the O−H bond of water molecules obtained by ultrafast infrared spectroscopy.[103] We also calculated the reorientation time of the O−H bond vector from the OACF of all the water molecules; the values of τ_2 in the first layer, obtained by fitting till 8 ps of correlation functions are 33.15, 5.12, 2.44, and 1.55 ps for 268, 298, 330, and 350 K, respectively. The orientational dynamics of water slow down significantly for supercooled water. With the decrease in temperature, we observe an increase in the reorientation time as the dynamics become slow. As evident from the classical molecular dynamics simulation study of the SPC/E model of water, the reduction of the temperature lowered the τ_2 of O−H reorientation vividly[104] in the supercooled region, and similar results were obtained within a temperature range of 310−210 K.[101]

Table 1. Values of Orientaional Relaxation Time Constant for i-HDW and i-LDW Molecules for Various Temperatures

temperature	region	A	τ_2 [ps]	β
268	layer 1	0.84	33.57	0.84
	layer 2	0.87	30.89	0.82
298	layer 1	0.84	5.14	0.79
	layer 2	0.86	4.48	0.78
330	layer 1	0.84	2.38	0.84
	layer 2	0.84	2.07	0.79
350	layer 1	0.84	1.58	0.89
	layer 2	0.82	1.42	0.85

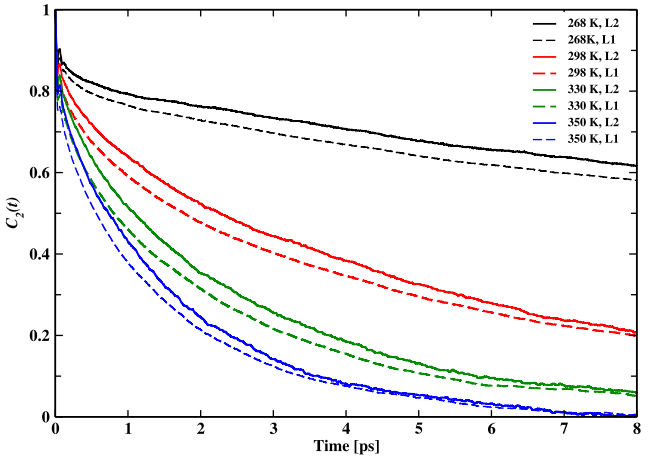

Figure 6. Second-order orientational correlation function of OH bonds in layers, L1 and L2 at different temperatures. Solid and dotted lines represent the correlation function of O−H bond vectors within the distance of 2.70 and the range of 2.70−3.35 Å, respectively.

3.6. Dynamics of i-LDW and i-HDW Molecules. We classified the two, three, and four coordinated water molecules as i-LDW, and five and above coordinated waters to be i-HDW. So, if a water molecule changes the coordination environments between dimer, trimer, and tetramer, it is considered to be in the instantaneous low-density zone, and if the coordination number is changed to 5 and above, it is considered to be in the instantaneous high-density zone. This definition can be appropriate as the frequent transition between these two types of water molecules usually occurs in a liquid state. We defined a coordination number variable $C_{cor}(t)$ for i-LDW as follows: If an oxygen molecule is continuously coordinated to 2, 3, or 4 oxygen atoms within a cut of 3.35 Å from time $t = 0$ to $t = t$, then $S(t) = 1$ or it is zero otherwise. The continuous coordination correlation function $C_{cor}(t)$ is defined as

$$C_{cor}(t) = \frac{\langle S(t)S(0)\rangle}{\langle S(0)^2\rangle} \tag{4}$$

Similarly, we calculated the $C_{cor}(t)$ for i-HDW as if an oxygen atom is continuously coordinated to five oxygen atoms or above within a cut of 3.35 Å from time $t = 0$ to $t = t$, then

https://dx.doi.org/10.1021/acs.jpcb.9b11596
J. Phys. Chem. B 2020, 124, 1071−1081

$S(t)$ = 1 or it is zero otherwise. The integrated time constant is the lifetime of the corresponding state of water. We show the decay of the correlation function in Figure 7. It can be seen

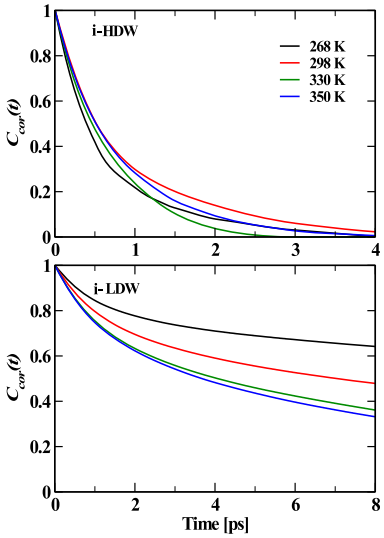

Figure 7. Coordination dynamics of i-HDW and i-LDW molecules at various temperatures.

that the lifetime of i-LDW is more for 268 K, and it decreases with the increase in the temperature, whereas the lifetime of i-HDW is more for 298 K. The calculated lifetime of these two types of molecules are tabulated in Table 2. We found that the

Table 2. Values of the Lifetimes of i-LDW and i-HDW Molecules at Various Temperatures

temperature (K)	$\tau_{\text{i-LDW}}$ (ps)	$\tau_{\text{i-HDW}}$ (ps)
268	23.16	0.70
298	13.03	0.97
330	11.24	0.67
350	10.21	0.82

lifetime of the low-density water molecule is much higher than that of the hydrogen bond lifetime of water. This lifetime can be related to the residence time of the water molecules.[73] It can be explained as such that making and breaking of hydrogen bonds can happen when a water molecule rotates even though, it is residing in the first solvation shell of the reference molecule. The lifetime of i-LDW molecules is much higher than the lifetime of the hydrogen bond and very much related to the residence time of a water molecule. However, the lifetime of the high-density water molecule is found to be less, even less than one ps. The interstitial water molecules are very much transient, and they change their positions between the first and second solvation shells very frequently. They are kind of intermediate water molecules that are in the process of transit from one solvation shell to the other solvation shell. However, their active participation in the process of hydrogen bond making and breaking affects the hydrogen bond lifetime and orientational relaxation time. Moreover, it was reported that the presence of i-HDW molecules in liquid water decreases the lifetime of the hydrogen bond.[31] The hydrogen bond dynamics of liquid water depends on the population of i-LDW and i-HDW. From the probability distribution of the population of two, three, four, and five coordinated water molecules, we find that the probability of finding five and more coordinated water molecules at 298 K is more than the other temperatures. The presence of more interstitial water molecules at 298 K decreases the hydrogen bond lifetime as well as the lifetime of i-LDW than 268 K, and it also increases the lifetime of i-HDW. At higher temperatures than 298 K, the probability of breaking of hydrogen bonds is more due to more thermal motion of water molecules. This reduces the probability of finding interstitial water molecules in the vicinity of the solvation shell, which makes the low probability of the existence of i-HDW and less lifetime of i-HDW. Therefore, we observe less lifetime of i-HDW for 330 and 350 K.

3.7. Frequency−Frequency Time Correlation Functions of OH Modes. From the earlier studies[34,62,66,67,71,73] of dynamics of frequency fluctuations in liquid water, it was observed that the frequency−frequency time correlation function has a short-time decay corresponding to the dynamics of intact hydrogen bonds and a longtime decay related to the average lifetime of hydrogen bonds, which was also confirmed by the lifetime obtained from the population correlation function approach. A recent study[74] related to temperature-dependent hydrogen bond lifetime, relaxation times of 3-pulse photon echo, and frequency−time correlation functions of water molecules using ab initio molecular dynamics simulations has been reported. The authors found that a strong correlation existed between the vibrational spectral diffusion timescale and hydrogen bond dynamics, and the timescale of vibrational spectral diffusion of the hydroxyl oscillator of water molecules slowed down with the decrease in temperature. The equilibrium distribution of the hydroxyl stretching frequencies gets blue-shifted with the increase of temperature. Therefore, in the current study, the environment around a water molecule can be very well understood by the vibrational spectral diffusion calculations. Keeping this in mind, we calculated the frequency−frequency correlation functions (Figure 8) of hydroxyl groups of water molecules by constructing two different layers. The first layer is considered up to a distance of 2.70 Å, and the second layer is considered to be till 3.35 Å to illustrate the effect of interstitial water

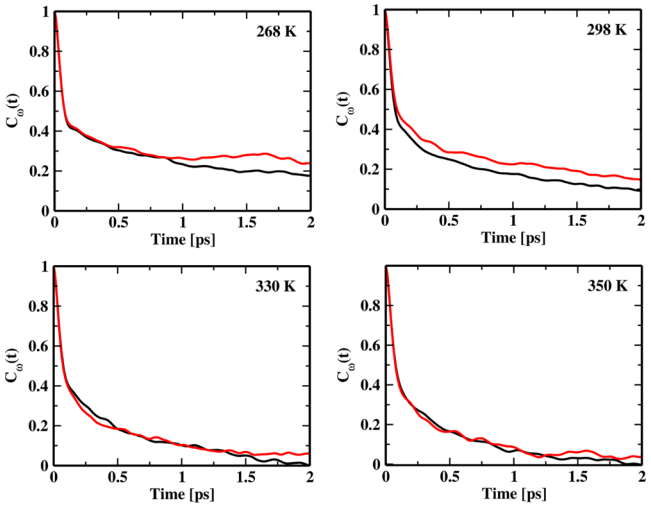

Figure 8. Frequency−frequency time correlation for the water molecules of layer 1 and layer 2 at different temperatures. Black and red colored lines represent the OH modes within the distance of 2.70 and within the range of 2.70−3.35 Å, respectively.

https://dx.doi.org/10.1021/acs.jpcb.9b11596
J. Phys. Chem. B 2020, 124, 1071−1081

molecules. The frequency−frequency time correlation function was calculated using the following equation

$$C_\omega(t) = \frac{\langle \delta\omega(t)\delta\omega(0)\rangle}{\langle \delta\omega(0)^2\rangle} \quad (5)$$

In this equation, $\delta\omega(t)$ is the fluctuation of the frequency from the average frequency at time t. The time constants for the decay of the frequency−frequency time correlation function was obtained by following tri-exponential function having an oscillation frequency term

$$f(t) = a_0 \cos(\omega_s t)e^{-t/\tau_0} + a_1 e^{-t/\tau_1} + (1 - a_0 - a_1)e^{-t/\tau_2} \quad (6)$$

This study is particularly important because it is well known that any change in thermodynamic conditions, such as a change in temperature and pressure, will affect the equilibrium between i-LDW and i-HDW molecules. The various time constants corresponding to frequency−frequency correlation functions obtained using eq 6 are shown in Table 3. It can be noted that there are mainly three different time scales: two short time scales and one long time scale. There is considerable weight in the coefficient of a short time scale. The three time scales can be related to the three different hydrogen bond lifetime of water. The first is due to i-HDW, second from the i-LDW structure, and third is due to the water molecules which are in transition between i-HDW and i-LDW. The long time scale τ_2 corresponds to the hydrogen bond lifetime of i-LDW. The short two time scales τ_0 and τ_1 can be related to the hydrogen bond lifetime due to i-HDW and the interfacial water molecules, which are in transition between i-HDW and i-LDW molecules. The τ_2 value of 268 K is found to be more than 298 K, which is further higher than that of 330 and 350 K.

Table 3. Spectral Diffusion Data for Layer 1 and Layer 2 Water Molecules for Various Temperatures

T [K]	layer	a_0	a_1	ω_s	τ_0	τ_1	τ_2
268	1	0.29	0.36	145.31	0.08	0.14	4.92
	2	0.29	0.37	142.05	0.07	0.13	4.96
298	1	0.24	0.41	136.96	0.08	0.12	1.68
	2	0.19	0.44	148.89	0.09	0.11	2.31
330	1	0.39	0.29	109.14	0.07	0.17	1.01
	2	0.24	0.44	138.22	0.08	0.12	0.93
350	1	0.27	0.45	108.76	0.08	0.12	0.78
	2	0.32	0.45	116.33	0.08	0.17	0.73

If we compare the coefficients and the time scales of layer 1 and layer 2 at 268 K, it can be found that the values a_0 and a_1 as well as τ_0, τ_1, and τ_2 are not very much different. This suggests that the environment of water molecules in layer 1 and layer 2 are not very much different at this temperature. At a higher temperature of 350 K, small changes in the τ_2 values are found. However, we notice a considerable amount of change in the τ_2 values at 298 K between the two layers. The composition of layer 1 and layer 2 changes a lot at ambient temperature. The coefficients, a_0 and a_1, also change a lot at this temperature, and the difference between τ_0 and τ_1 values becomes very less for layer 2, suggesting the bi-exponential decay of the frequency−frequency correlation function. The hydrogen bond lifetime of i-HDW and transiting water molecules between i-LDW and i-HDW molecules (intermediate step) becomes almost equal at 298 K. The transition between the i-LDW and i-HDW molecules is so quick that their time scales become inseparable with the i-HDW at this temperature. This may be due to the presence of a considerable amount of interstitial water molecules at this temperature. The change in the composition of the i-HDW and interfacial (i-HDW−i-LDW) water molecules (a_0 = 0.19, a_1 = 0.44) contributes toward the increase in the value of τ_2 for layer 2. At higher temperatures, 330 K, we find a slight decrease in the τ_2 values for layer 2 due to the presence of the interstitial water molecules in this layer. Therefore, the anomalous property of water can be related to the presence of more tetrahedral and interstitial water molecules. It will become clearer if we study the dependence of the hydrogen bond lifetime, dangling lifetime, and the population of i-HDW at various temperatures, which are presented in Figure 9 for a comparison. The slight increase in the lifetime of dangling hydroxyl bonds is observed with an increase in temperature. More importantly, we observe a crossover point between values of the hydrogen bond and dangling lifetime and maximum population of i-HDW at 298 K.

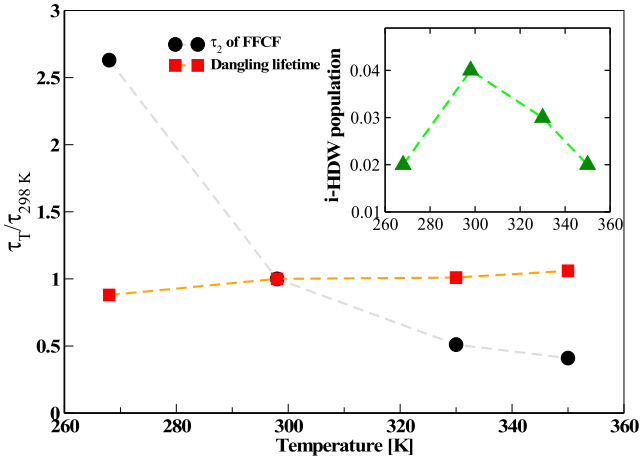

Figure 9. Variation of the ratio of hydrogen bond lifetime (from FFCF), dangling lifetime at different temperatures, and the values at 298 K. In the inset, we show the variation of i-HDW population with temperature. The values of hydrogen bond and dangling OH lifetime are 1.84 and 0.068 ps, respectively.

4. CONCLUSIONS

To summarize, we have investigated the effect of temperatures on density, structure, spectra, voids, and interstitial molecules of water in the liquid phase from FPMD simulations. The thermophysical properties, like density, cohesive energy, and isothermal compressibility, were also calculated at various temperatures. The minimum in compressibility values were found to correlate with the maxima in density and cohesive energy at 298 K. At lower temperatures, compact first and second solvation shells were found. The anomalous property of water can be related to the distinctive presence of the interstitial water molecules, which mix up with the first and second solvation shell when the temperature is increased. The orientational profile and vibrational spectral dynamics were analyzed considering two layers of water molecules where the heterogeneous density was found. The heterogeneity in density facilitates the existence of i-HDW and i-LDW molecules. The water molecules in layer 1 showed slower orientational dynamics of OH bonds than that of layer 2 for all the temperatures. However, at higher temperatures, 330 and 350

https://dx.doi.org/10.1021/acs.jpcb.9b11596
J. Phys. Chem. B 2020, 124, 1071−1081

K, water molecules in layer 1 have almost the same orientational lifetime as of layer 2; they become indistinguishable. We have also seen from the distribution of the voids that at 268 K, there is a shift toward the higher value of the radius of vacancies than other temperatures; the water molecules are predominately in the i-LDW region as compared to the other temperatures. At 298 K, the radius of vacancies is found to be least, which suggests a maximum population of i-HDW. The population of these i-HDW decreases from 298 to 350 K. The lifetime of the i-LDW water molecules is maximum at 268 K, and it decreases with the increase in the temperature. However, the lifetime of the i-HDW water molecules was found to a maximum at 298 K. We analyzed spectral diffusion in terms of layer 1 and layer 2 water molecules. On plotting hydrogen bond lifetime and dangling lifetime, we found a crossover region near 298 K, where we have a maximum population of i-HDW. The behavior of the interstitial molecules at 298 K is unique compared to the other temperatures. Their population is more at 298 K, and the hydrogen bond lifetime is also more in layer 2. Therefore, it can be concluded that the anomalous thermophysical properties observed for water molecules may be due to the presence of interstitial water molecules, which facilitate the structural and dynamical rearrangement inside the three-dimensional network of hydrogen bonds according to the available physical conditions.

AUTHOR INFORMATION

Corresponding Authors

Debashree Chakraborty − *Department of Chemistry, National Institute of Technology Karnataka, 575025 Mangalore, India;* orcid.org/0000-0002-0142-7941; Phone: +91 824 2473212; Email: debashree@nitk.edu.in

Bhabani S. Mallik − *Department of Chemistry, Indian Institute of Technology Hyderabad, Kandi-502285 Sangareddy, India;* orcid.org/0000-0001-9657-1497; Phone: +91 40 2301 7051; Email: bhabani@iith.ac.in

Authors

Adyasa Priyadarshini − *Department of Chemistry, Indian Institute of Technology Hyderabad, Kandi-502285 Sangareddy, India*

Aritri Biswas − *Department of Chemistry, Indian Institute of Technology Hyderabad, Kandi-502285 Sangareddy, India*

Complete contact information is available at: https://pubs.acs.org/10.1021/acs.jpcb.9b11596

Author Contributions

[§]A.P. and A.B. equally contributed.

Notes

The authors declare no competing financial interest.

ACKNOWLEDGMENTS

Funding from the Department of Science and Technology (DST), India (EMR/2016/004965), for B.S.M. is acknowledged. A.B. and A.P. like to acknowledge MHRD, India, for their Ph.D. fellowship. The authors also thank Dr. Sohag Biswas for his help during the preparation of the manuscript.

REFERENCES

(1) Franks, F. *Water A Comprehensive Treatise: Volume 4: Aqueous Solutions of Amphiphiles and Macromolecules*; Springer US, 1975.

(2) Kell, G. S. Isothermal Compressibility of Liquid Water at 1 Atm. *J. Chem. Eng. Data* **1970**, *15*, 119−122.

(3) Speedy, R. J.; Angell, C. A. Isothermal Compressibility of Supercooled Water and Evidence for a Thermodynamic Singularity at −45°C. *J. Chem. Phys.* **1976**, *65*, 851−858.

(4) Stanley, H. E.; Teixeira, J. Interpretation of the Unusual Behavior of H2O and D2O at Low Temperatures: Tests of a Percolation Model. *J. Chem. Phys.* **1980**, *73*, 3404−3422.

(5) Moore, E. B.; Molinero, V. Structural Transformation in Supercooled Water Controls the Crystallization Rate of Ice. *Nature* **2011**, *479*, 506−508.

(6) Woutersen, S.; Emmerichs, U.; Bakker, H. J. Femtosecond Mid-IR Pump-Probe Spectroscopy of Liquid Water: Evidence for a Two-Component Structure. *Science* **1997**, *278*, 658−660.

(7) Laenen, R.; Rauscher, C.; Laubereau, A. Dynamics of Local Substructures in Water Observed by Ultrafast Infrared Hole Burning. *Phys. Rev. Lett.* **1998**, *80*, 2622−2625.

(8) Stillinger, F. H. Water Revisited. *Science* **1980**, *209*, 451−457.

(9) Soper, A. K. Orientational Correlation Function for Molecular Liquids: The Case of Liquid Water. *J. Chem. Phys.* **1994**, *101*, 6888−6901.

(10) Kuharski, R. A.; Rossky, P. J. A Quantum Mechanical Study of Structure in Liquid H2O and D2O. *J. Chem. Phys.* **1985**, *82*, 5164−5177.

(11) Luzar, A.; Chandler, D. Effect of Environment on Hydrogen Bond Dynamics in Liquid Water. *Phys. Rev. Lett.* **1996**, *76*, 928−931.

(12) Soper, A. K.; Ricci, M. A. Structures of High-Density and Low-Density Water. *Phys. Rev. Lett.* **2000**, *84*, 2881−2884.

(13) Mahoney, M. W.; Jorgensen, W. L. A Five-Site Model for Liquid Water and the Reproduction of the Density Anomaly by Rigid, Nonpolarizable Potential Functions. *J. Chem. Phys.* **2000**, *112*, 8910−8922.

(14) Shiratani, E.; Sasai, M. Growth and Collapse of Structural Patterns in the Hydrogen Bond Network in Liquid Water. *J. Chem. Phys.* **1996**, *104*, 7671−7680.

(15) Shiratani, E.; Sasai, M. Molecular Scale Precursor of the Liquid−Liquid Phase Transition of Water. *J. Chem. Phys.* **1998**, *108*, 3264−3276.

(16) Jana, B.; Bagchi, B. Intermittent Dynamics, Stochastic Resonance and Dynamical Heterogeneity in Supercooled Liquid Water. *J. Phys. Chem. B* **2009**, *113*, 2221−2224.

(17) Johari, G. P.; Teixeira, J. Thermodynamic Analysis of the Two-Liquid Model for Anomalies of Water, HDL−LDL Fluctuations, and Liquid−Liquid Transition. *J. Phys. Chem. B* **2015**, *119*, 14210−14220.

(18) Sciortino, F.; Fornili, S. L. Hydrogen Bond Cooperativity in Simulated Water: Time Dependence Analysis of Pair Interactions. *J. Chem. Phys.* **1989**, *90*, 2786−2792.

(19) Stirnemann, G.; Laage, D. Communication: On the Origin of the Non-Arrhenius Behavior in Water Reorientation Dynamics. *J. Chem. Phys.* **2012**, *137*, 031101.

(20) Poole, P. H.; Sciortino, F.; Essmann, U.; Stanley, H. E. Phase Behaviour of Metastable Water. *Nature* **1992**, *360*, 324−328.

(21) Moynihan, C. T. Two Species/Nonideal Solution Model for Amorphous/Amorphous Phase Transitions. *MRS Online Proc. Libr.* **1996**, *455*, 411.

(22) Mishima, O.; Stanley, H. E. Decompression-Induced Melting of Ice IV and the Liquid−Liquid Transition in Water. *Nature* **1998**, *392*, 164−168.

(23) Vega, C.; Abascal, J. L. F. Relation between the Melting Temperature and the Temperature of Maximum Density for the Most Common Models of Water. *J. Chem. Phys.* **2005**, *123*, 144504.

(24) Wernet, P.; Nordlund, D.; Bergmann, U.; Cavalleri, M.; Odelius, M.; Ogasawara, H.; Näslund, L. Å.; Hirsch, T. K.; Ojamäe, L.; Glatzel, P.; et al. The Structure of the First Coordination Shell in Liquid Water. *Science* **2004**, *304*, 995−999.

(25) Head-Gordon, T.; Johnson, M. E. Tetrahedral Structure or Chains for Liquid Water. *Proc. Natl. Acad. Sci. U.S.A.* **2006**, *103*, 7973−7977.

(26) Huang, C.; Wikfeldt, K. T.; Tokushima, T.; Nordlund, D.; Harada, Y.; Bergmann, U.; Niebuhr, M.; Weiss, T. M.; Horikawa, Y.; Leetmaa, M.; et al. The Inhomogeneous Structure of Water at Ambient Conditions. *Proc. Natl. Acad. Sci. U.S.A.* **2009**, *106*, 15214−15218.
(27) Bellissent-Funel, M.-C. Is There a Liquid-Liquid Phase Transition in Supercooled Water? *EPL* **1998**, *42*, 161.
(28) Rønne, C.; Åstrand, P.-O.; Keiding, S. R. THz Spectroscopy of Liquid H2O and D2O. *Phys. Rev. Lett.* **1999**, *82*, 2888−2891.
(29) Fanetti, S.; Lapini, A.; Pagliai, M.; Citroni, M.; Di Donato, M.; Scandolo, S.; Righini, R.; Bini, R. Structure and Dynamics of Low-Density and High-Density Liquid Water at High Pressure. *J. Phys. Chem. Lett.* **2014**, *5*, 235−240.
(30) Ansari, N.; Dandekar, R.; Caravati, S.; Sosso, G. c.; Hassanali, A. High and Low Density Patches in Simulated Liquid Water. *J. Chem. Phys.* **2018**, *149*, 204507.
(31) Biswas, S.; Chakraborty, D.; Mallik, B. S. Interstitial Voids and Resultant Density of Liquid Water: A First-Principles Molecular Dynamics Study. *ACS Omega* **2018**, *3*, 2010−2017.
(32) Naserifar, S.; Goddard, W. A. Liquid Water Is a Dynamic Polydisperse Branched Polymer. *Proc. Natl. Acad. Sci. U.S.A.* **2019**, *116*, 1998−2003.
(33) Lawrence, C. P.; Skinner, J. L. Ultrafast Infrared Spectroscopy Probes Hydrogen-Bonding Dynamics in Liquid Water. *Chem. Phys. Lett.* **2003**, *369*, 472−477.
(34) Rey, R.; Møller, K. B.; Hynes, J. T. Hydrogen Bond Dynamics in Water and Ultrafast Infrared Spectroscopy. *J. Phys. Chem. A* **2002**, *106*, 11993−11996.
(35) Jimenez, R.; Fleming, G. R.; Kumar, P. V.; Maroncelli, M. Femtosecond Solvation Dynamics of Water. *Nature* **1994**, *369*, 471−473.
(36) Ohmine, I.; Saito, S. Water Dynamics: Fluctuation, Relaxation, and Chemical Reactions in Hydrogen Bond Network Rearrangement. *Acc. Chem. Res.* **1999**, *32*, 741−749.
(37) Nienhuys, H.-K.; van Santen, R. A.; Bakker, H. J. Orientational Relaxation of Liquid Water Molecules as an Activated Process. *J. Chem. Phys.* **2000**, *112*, 8487−8494.
(38) Bakker, H. J.; Woutersen, S.; Nienhuys, H.-K. Reorientational Motion and Hydrogen-Bond Stretching Dynamics in Liquid Water. *Chem. Phys.* **2000**, *258*, 233−245.
(39) Gallot, G.; Bratos, S.; Pommeret, S.; Lascoux, N.; Leicknam, J.-C.; Koziński, M.; Amir, W.; Gale, G. M. Coupling between molecular rotations and OH···O motions in liquid water: Theory and experiment. *J. Chem. Phys.* **2002**, *117*, 11301−11309.
(40) Rezus, Y. L. A.; Bakker, H. J. On the Orientational Relaxation of HDO in Liquid Water. *J. Chem. Phys.* **2005**, *123*, 114502.
(41) Rezus, Y. L. A.; Bakker, H. J. Orientational Dynamics of Isotopically Diluted H2O and D2O. *J. Chem. Phys.* **2006**, *125*, 144512.
(42) Graener, H.; Seifert, G.; Laubereau, A. New Spectroscopy of Water Using Tunable Picosecond Pulses in the Infrared. *Phys. Rev. Lett.* **1991**, *66*, 2092−2095.
(43) Gale, G. M.; Gallot, G.; Hache, F.; Lascoux, N.; Bratos, S.; Leicknam, J.-C. Femtosecond Dynamics of Hydrogen Bonds in Liquid Water: A Real Time Study. *Phys. Rev. Lett.* **1999**, *82*, 1068−1071.
(44) Woutersen, S.; Bakker, H. J. Hydrogen Bond in Liquid Water as a Brownian Oscillator. *Phys. Rev. Lett.* **1999**, *83*, 2077−2080.
(45) Bakker, H. J.; Nienhuys, H.-K.; Gallot, G.; Lascoux, N.; Gale, G. M.; Leicknam, J.-C.; Bratos, S. Transient Absorption of Vibrationally Excited Water. *J. Chem. Phys.* **2002**, *116*, 2592−2598.
(46) Cho, M.; Yu, J.-Y.; Joo, T.; Nagasawa, Y.; Passino, S. A.; Fleming, G. R. The Integrated Photon Echo and Solvation Dynamics. *J. Phys. Chem.* **1996**, *100*, 11944−11953.
(47) Piryatinski, A.; Skinner, J. L. Determining Vibrational Solvation-Correlation Functions from Three-Pulse Infrared Photon Echoes. *J. Phys. Chem. B* **2002**, *106*, 8055−8063.
(48) Fecko, C. J.; Eaves, J. D.; Loparo, J. J.; Tokmakoff, A.; Geissler, P. L. Ultrafast Hydrogen-Bond Dynamics in the Infrared Spectroscopy of Water. *Science* **2003**, *301*, 1698−1702.
(49) Fecko, C. J.; Loparo, J. J.; Roberts, S. T.; Tokmakoff, A. Local Hydrogen Bonding Dynamics and Collective Reorganization in Water: Ultrafast Infrared Spectroscopy of HOD/D2O. *J. Chem. Phys.* **2005**, *122*, 054506.
(50) Stenger, J.; Madsen, D.; Hamm, P.; Nibbering, E. T. J.; Elsaesser, T. A Photon Echo Peak Shift Study of Liquid Water. *J. Phys. Chem. A* **2002**, *106*, 2341−2350.
(51) Eaves, J. D.; Loparo, J. J.; Fecko, C. J.; Roberts, S. T.; Tokmakoff, A.; Geissler, P. L. Hydrogen Bonds in Liquid Water Are Broken Only Fleetingly. *Proc. Natl. Acad. Sci. U.S.A.* **2005**, *102*, 13019−13022.
(52) Asbury, J. B.; Steinel, T.; Stromberg, C.; Corcelli, S. A.; Lawrence, C. P.; Skinner, J. L.; Fayer, M. D. Water Dynamics: Vibrational Echo Correlation Spectroscopy and Comparison to Molecular Dynamics Simulations. *J. Phys. Chem. A* **2004**, *108*, 1107−1119.
(53) Roberts, S. T.; Loparo, J. J.; Tokmakoff, A. Characterization of Spectral Diffusion from Two-Dimensional Line Shapes. *J. Chem. Phys.* **2006**, *125*, 084502.
(54) Kwak, K.; Park, S.; Finkelstein, I. J.; Fayer, M. D. Frequency-Frequency Correlation Functions and Apodization in Two-Dimensional Infrared Vibrational Echo Spectroscopy: A New Approach. *J. Chem. Phys.* **2007**, *127*, 124503.
(55) Steinel, T.; Asbury, J. B.; Corcelli, S. A.; Lawrence, C. P.; Skinner, J. L.; Fayer, M. D. Water Dynamics: Dependence on Local Structure Probed with Vibrational Echo Correlation Spectroscopy. *Chem. Phys. Lett.* **2004**, *386*, 295−300.
(56) Asbury, J. B.; Steinel, T.; Kwak, K.; Corcelli, S. A.; Lawrence, C. P.; Skinner, J. L.; Fayer, M. D. Dynamics of Water Probed with Vibrational Echo Correlation Spectroscopy. *J. Chem. Phys.* **2004**, *121*, 12431−12446.
(57) Loparo, J. J.; Roberts, S. T.; Tokmakoff, A. Multidimensional Infrared Spectroscopy of Water. I. Vibrational Dynamics in Two-Dimensional IR Line Shapes. *J. Chem. Phys.* **2006**, *125*, 194521.
(58) Loparo, J. J.; Roberts, S. T.; Tokmakoff, A. Multidimensional Infrared Spectroscopy of Water. II. Hydrogen Bond Switching Dynamics. *J. Chem. Phys.* **2006**, *125*, 194522.
(59) Yeremenko, S.; Pshenichnikov, M. S.; Wiersma, D. A. Hydrogen-Bond Dynamics in Water Explored by Heterodyne-Detected Photon Echo. *Chem. Phys. Lett.* **2003**, *369*, 107−113.
(60) Stenger, J.; Madsen, D.; Hamm, P.; Nibbering, E. T. J.; Elsaesser, T. A Photon Echo Peak Shift Study of Liquid Water. *J. Phys. Chem. A* **2002**, *106*, 2341−2350.
(61) Lawrence, C. P.; Skinner, J. L. Vibrational Spectroscopy of HOD in Liquid D2O. II. Infrared Line Shapes and Vibrational Stokes Shift. *J. Chem. Phys.* **2002**, *117*, 8847−8854.
(62) Lawrence, C. P.; Skinner, J. L. Vibrational Spectroscopy of HOD in Liquid D2O. III. Spectral Diffusion, and Hydrogen-Bonding and Rotational Dynamics. *J. Chem. Phys.* **2003**, *118*, 264−272.
(63) Piryatinski, A.; Lawrence, C. P.; Skinner, J. L. Vibrational Spectroscopy of HOD in Liquid D2O. IV. Infrared Two-Pulse Photon Echoes. *J. Chem. Phys.* **2003**, *118*, 9664−9671.
(64) Piryatinski, A.; Lawrence, C. P.; Skinner, J. L. Vibrational Spectroscopy of HOD in Liquid D2O. V. Infrared Three-Pulse Photon Echoes. *J. Chem. Phys.* **2003**, *118*, 9672−9679.
(65) Corcelli, S. A.; Lawrence, C. P.; Asbury, J. B.; Steinel, T.; Fayer, M. D.; Skinner, J. L. Spectral Diffusion in a Fluctuating Charge Model of Water. *J. Chem. Phys.* **2004**, *121*, 8897−8900.
(66) Corcelli, S. A.; Lawrence, C. P.; Skinner, J. L. Combined Electronic Structure/Molecular Dynamics Approach for Ultrafast Infrared Spectroscopy of Dilute HOD in Liquid H2O and D2O. *J. Chem. Phys.* **2004**, *120*, 8107−8117.
(67) Møller, K. B.; Rey, R.; Hynes, J. T. Hydrogen Bond Dynamics in Water and Ultrafast Infrared Spectroscopy: A Theoretical Study. *J. Phys. Chem. A* **2004**, *108*, 1275−1289.
(68) Hayashi, T.; la Cour Jansen, T.; Zhuang, W.; Mukamel, S. Collective Solvent Coordinates for the Infrared Spectrum of HOD in D2O Based on an Ab Initio Electrostatic Map. *J. Phys. Chem. A* **2005**, *109*, 64−82.

https://dx.doi.org/10.1021/acs.jpcb.9b11596
J. Phys. Chem. B 2020, 124, 1071−1081

(69) Eaves, J. D.; Tokmakoff, A.; Geissler, P. L. Electric Field Fluctuations Drive Vibrational Dephasing in Water. *J. Phys. Chem. A* **2005**, *109*, 9424−9436.
(70) Schmidt, J. R.; Corcelli, S. A.; Skinner, J. L. Pronounced Non-Condon Effects in the Ultrafast Infrared Spectroscopy of Water. *J. Chem. Phys.* **2005**, *123*, 044513.
(71) Schmidt, J. R.; Roberts, S. T.; Loparo, J. J.; Tokmakoff, A.; Fayer, M. D.; Skinner, J. L. Are Water Simulation Models Consistent with Steady-State and Ultrafast Vibrational Spectroscopy Experiments? *Chem. Phys.* **2007**, *341*, 143−157.
(72) Auer, B.; Kumar, R.; Schmidt, J. R.; Skinner, J. L. Hydrogen Bonding and Raman, IR, and 2D-IR Spectroscopy of Dilute HOD in Liquid D2O. *Proc. Natl. Acad. Sci. U.S.A.* **2007**, *104*, 14215−14220.
(73) Mallik, B. S.; Semparithi, A.; Chandra, A. Vibrational Spectral Diffusion and Hydrogen Bond Dynamics in Heavy Water from First Principles. *J. Phys. Chem. A* **2008**, *112*, 5104−5112.
(74) Ojha, D.; Chandra, A. Temperature Dependence of the Ultrafast Vibrational Echo Spectroscopy of OD Modes in Liquid Water from First Principles Simulations. *Phys. Chem. Chem. Phys.* **2019**, *21*, 6485−6498.
(75) Becke, A. D. Density-Functional Exchange-Energy Approximation with Correct Asymptotic Behavior. *Phys. Rev. A: At., Mol., Opt. Phys.* **1988**, *38*, 3098−3100.
(76) Lee, C.; Yang, W.; Parr, R. G. Development of the Colle-Salvetti Correlation-Energy Formula into a Functional of the Electron Density. *Phys. Rev. B: Condens. Matter Mater. Phys.* **1988**, *37*, 785−789.
(77) Grimme, S.; Antony, J.; Ehrlich, S.; Krieg, H. A Consistent and Accurate Ab Initio Parametrization of Density Functional Dispersion Correction (DFT-D) for the 94 Elements H-Pu. *J. Chem. Phys.* **2010**, *132*, 154104.
(78) Hutter, J.; Iannuzzi, M.; Schiffmann, F.; VandeVondele, J. Cp2k: Atomistic Simulations of Condensed Matter Systems. *Wiley Interdiscip. Rev.: Comput. Mol. Sci.* **2014**, *4*, 15−25.
(79) Hutter, J.; Iannuzzi, M.; Schiffmann, F.; VandeVondele, J. Cp2k: Atomistic Simulations of Condensed Matter Systems. *Wiley Interdiscip. Rev.: Comput. Mol. Sci.* **2014**, *4*, 15−25.
(80) Goedecker, S.; Teter, M.; Hutter, J. Separable Dual-Space Gaussian Pseudopotentials. *Phys. Rev. B: Condens. Matter Mater. Phys.* **1996**, *54*, 1703−1710.
(81) Hartwigsen, C.; Goedecker, S.; Hutter, J. Relativistic Separable Dual-Space Gaussian Pseudopotentials from H to Rn. *Phys. Rev. B: Condens. Matter Mater. Phys.* **1998**, *58*, 3641−3662.
(82) Jonchiere, R.; Seitsonen, A. P.; Ferlat, G.; Saitta, A. M.; Vuilleumier, R. Van Der Waals Effects in Ab Initio Water at Ambient and Supercritical Conditions. *J. Chem. Phys.* **2011**, *135*, 154503.
(83) Berendsen, H. J. C.; Grigera, J. R.; Straatsma, T. P. The Missing Term in Effective Pair Potentials. *J. Phys. Chem.* **1987**, *91*, 6269−6271.
(84) Martyna, G. J.; Klein, M. L.; Tuckerman, M. Nosé-Hoover chains: The canonical ensemble via continuous dynamics. *J. Chem. Phys.* **1992**, *97*, 2635−2643.
(85) Schmidt, J.; VandeVondele, J.; Kuo, I.-F. W.; Sebastiani, D.; Siepmann, J. I.; Hutter, J.; Mundy, C. J. Isobaric−Isothermal Molecular Dynamics Simulations Utilizing Density Functional Theory: An Assessment of the Structure and Density of Water at Near-Ambient Conditions. *J. Phys. Chem. B* **2009**, *113*, 11959−11964.
(86) Nilsson, A.; Pettersson, L. G. M. The Structural Origin of Anomalous Properties of Liquid Water. *Nat. Commun.* **2015**, *6*, 8998.
(87) Pettersson, L. G. M.; Henchman, R. H.; Nilsson, A. Water—The Most Anomalous Liquid. *Chem. Rev.* **2016**, *116*, 7459−7462.
(88) Kell, G. S. Density, Thermal Expansivity, and Compressibility of Liquid Water from 0 Deg. to 150 Deg. Correlations and Tables for Atmospheric Pressure and Saturation Reviewed and Expressed on 1968 Temperature Scale. *J. Chem. Eng. Data* **1975**, *20*, 97−105.
(89) Sun, C. Q.; Wang, Y.; Tay, B. K.; Li, S.; Huang, H.; Zhang, Y. B. Correlation between the Melting Point of a Nanosolid and the Cohesive Energy of a Surface Atom. *J. Phys. Chem. B* **2002**, *106*, 10701−10705.
(90) Sokhan, V. P.; Jones, A. P.; Cipcigan, F. S.; Crain, J.; Martyna, G. J. Signature Properties of Water: Their Molecular Electronic Origins. *Proc. Natl. Acad. Sci. U.S.A.* **2015**, *112*, 6341−6346.
(91) Lovelock, K. R. J. Quantifying Intermolecular Interactions of Ionic Liquids Using Cohesive Energy Densities. *R. Soc. Open Sci.* **2017**, *4*, 171223.
(92) Kirkham, M. B. 3—Structure and Properties of Water. In *Principles of Soil and Plant Water Relations*; Kirkham, M. B., Ed.; Academic Press: Burlington, 2005; pp 27−40.
(93) Fine, R. A.; Millero, F. J. Compressibility of Water as a Function of Temperature and Pressure. *J. Chem. Phys.* **1973**, *59*, 5529−5536.
(94) Gaiduk, A. P.; Gygi, F.; Galli, G. Density and Compressibility of Liquid Water and Ice from First-Principles Simulations with Hybrid Functionals. *J. Phys. Chem. Lett.* **2015**, *6*, 2902−2908.
(95) Soper, A. K. The Radial Distribution Functions of Water and Ice from 220 to 673 K and at Pressures up to 400 MPa. *Chem. Phys.* **2000**, *258*, 121−137.
(96) Skinner, L. B.; Huang, C.; Schlesinger, D.; Pettersson, L. G. M.; Nilsson, A.; Benmore, C. J. Benchmark Oxygen-Oxygen Pair-Distribution Function of Ambient Water from x-Ray Diffraction Measurements with a Wide Q-Range. *J. Chem. Phys.* **2013**, *138*, 074506.
(97) Smith, J. D.; Cappa, C. D.; Wilson, K. R.; Messer, B. M.; Cohen, R. C.; Saykally, R. J. Energetics of Hydrogen Bond Network Rearrangements in Liquid Water. *Science* **2004**, *306*, 851−853.
(98) Tan, M.-L.; Fischer, J. T.; Chandra, A.; Brooks, B. R.; Ichiye, T. A Temperature of Maximum Density in Soft Sticky Dipole Water. *Chem. Phys. Lett.* **2003**, *376*, 646−652.
(99) Chakraborty, D.; Chandra, A. An Analysis of Voids and Necks in Supercritical Water. *J. Mol. Liq.* **2011**, *163*, 1−6.
(100) Chakraborty, D.; Chandra, A. Voids and Necks in Liquid Ammonia and Their Roles in Diffusion of Ions of Varying Size. *J. Comput. Chem.* **2012**, *33*, 843−852.
(101) Kumar, P.; Franzese, G.; Buldyrev, S. V.; Stanley, H. E. Molecular Dynamics Study of Orientational Cooperativity in Water. *Phys. Rev. E: Stat., Nonlinear, Soft Matter Phys.* **2006**, *73*, 041505.
(102) Stirnemann, G.; Duboué-Dijon, E.; Laage, D. Ab Initio Simulations of Water Dynamics in Aqueous TMAO Solutions: Temperature and Concentration Effects. *J. Phys. Chem. B* **2017**, *121*, 11189−11197.
(103) Rezus, Y. L. A.; Bakker, H. J. On the Orientational Relaxation of HDO in Liquid Water. *J. Chem. Phys.* **2005**, *123*, 114502.
(104) Netz, P. A.; Starr, F.; Barbosa, M. C.; Stanley, H. E. Translational and Rotational Diffusion in Stretched Water. *J. Mol. Liq.* **2002**, *101*, 159−168.

https://dx.doi.org/10.1021/acs.jpcb.9b11596
J. Phys. Chem. B 2020, 124, 1071−1081